AFRL-RW-EG-TP-2010-071

MODELING SOLID STATE DETONATION AND REACTIVE MATERIALS

David E. Lambert,
Air Force Research Laboratory
Munitions Directorate
AFRL/RWMW
Eglin AFB, FL 32542-6810

Sunhee Yoo
D. Scott Stewart
University of Illinois
Urbana, IL 61801

JULY 2010

SYMPOSIUM PAPER

This paper has been submitted to the Office of Naval Research and the International Detonation Symposium Organizing Committee, and has been presented at the 2010 International Detonation Symposium.

AIR FORCE RESEARCH LABORATORY
MUNITIONS DIRECTORATE

■ **Air Force Materiel Command** ■ **United States Air Force** ■ **Eglin Air Force Base, FL 32542**

REPORT DOCUMENTATION PAGE

Form Approved
OMB No. 0704-0188

PLEASE DO NOT RETURN YOUR FORM TO THE ABOVE ADDRESS.

1. REPORT DATE *(DD-MM-YYYY)*	2. REPORT TYPE	3. DATES COVERED *(From - To)*
07-2010	Symposium Paper	

4. TITLE AND SUBTITLE

Modeling Solid State Detonation and Reactive Materials

5a. CONTRACT NUMBER

N/A

5b. GRANT NUMBER

N/A

5c. PROGRAM ELEMENT NUMBER

N/A

6. AUTHOR(S)

1. David E. Lambert (AFRL/RWMW)
2. Sunhee Yoo
3. D. Scott Stewart

5d. PROJECT NUMBER

4347

5e. TASK NUMBER

92

5f. WORK UNIT NUMBER

00

7. PERFORMING ORGANIZATION NAME(S) AND ADDRESS(ES)

1. Air Force Research Laboratory
Munitions Directorate
AFRL/RWMW
Eglin AFB, FL 32542-6810

2. University of Illinois
Urbana, IL 61801

8. PERFORMING ORGANIZATION REPORT NUMBER

AFRL-RW-EG-TP-2010-071

9. SPONSORING/MONITORING AGENCY NAME(S) AND ADDRESS(ES)

Air Force Research Laboratory
Munitions Directorate
AFRL/RWMW
Eglin AFB, FL 32542-6810

10. SPONSOR/MONITOR'S ACRONYM(S)

AFRL-RW-EG

11. SPONSOR/MONITOR'S REPORT NUMBER(S)

SAME AS BLOCK 8

12. DISTRIBUTION/AVAILABILITY STATEMENT

DISTRIBUTION A: Approved for public release; distribution unlimited. Approval Confirmation 96 ABW/PA# 96ABW-2010-0248 dated 15 April 2010.

13. SUPPLEMENTARY NOTES

See 'cover page' for pertinent metadata information.

14. ABSTRACT

Solid state detonation (SSD) refers to non-classical phenomena whereby chemical reaction sustains a self-propagation wave in energetic materials that are not typically considered explosives. This wave phenomenon can be observed when fast 'shock induced' reactions occur as the result of deformation during the crush-up of the powders to their full density. We demonstrate that SSD, modeled with a simple phenomenological model, nominally runs at pressures much lower than what is observed in "ideal" explosives. However the lead wave head is not a classical shock in the sense of ZND theory, but rather a subsonic compaction wave. Hence the SSD is not strictly steady but rather quasi-steady. Analytical results from steady wave analysis are confirmed by direct simulation that includes the transients of the transition to quasi-steady self sustained reaction applied to a mixture of aluminum-Teflon reactive material.

15. SUBJECT TERMS

16. SECURITY CLASSIFICATION OF:			17. LIMITATION OF ABSTRACT	18. NUMBER OF PAGES	19a. NAME OF RESPONSIBLE PERSON
a. REPORT	b. ABSTRACT	c. THIS PAGE			David E. Lambert
UNCLASSIFIED	UNCLASSIFIED	UNCLASSIFIED	SAR	8	19b. TELEPHONE NUMBER *(Include area code)* 850-882-7991

MODELING SOLID STATE DETONATION AND REACTIVE MATERIALS

Sunhee Yoo[†], Scott D. Stewart[†], David E. Lambert[‡], Mark A. Lieber[†] and Matthew J. Szuck[†]

[†]Mechanical Science and Engineering, University of Illinois, Urbana, IL 61801
[‡]Air Force Research Laboratory, Munitions Directorate, Eglin AFB, 32542

Abstract. Solid state detonation (SSD) refers to non-classical phenomena whereby chemical reaction sustains a self-propagation wave in energetic materials that are not typically considered explosives. This wave phenomenon can be observed when fast 'shock induced' reactions occur as the result of deformation during the crush-up of the powders to their full density [3]. We demonstrate that SSD, modeled with a simple phenomenological model, nominally runs at pressures much lower than what is observed in "ideal" explosives. However the lead wave head is not a classical shock in the sense of ZND theory, but rather a subsonic compaction wave. Hence the SSD is not strictly steady but rather quasi-steady. Analytical results from steady wave analysis are confirmed by direct simulation that includes the transients of the transition to quasi-steady self sustained reaction applied to a mixture of aluminum-Teflon reactive material.

Introduction

In this paper we describe a simple model for the phenomenological study of solid state detonation, which is a description of non-classical detonation wave phenomena in porous mixtures of reactive materials. For the purposes of illustration we consider a reactive material that is made from a meso-scale mixture of aluminum with Telfon oxidizer.

We are especially interested in ignition phenomena and the possibility of transition to detonation in these materials that may have varied mass ratios of reactant materials, packing densities in relation to theoretical maximum density, (TMD), which are design inputs. In this paper, the detailed composition of a mixture, rates of pore-collapse, and reaction are modeled specifically without specifying the detailed properties of resulting reacted products. But those details can be included by allowing for more complex macroscopic constitutive theory that derives from meso-scopic modeling. This model is intended to be a framework from which one can evaluate the macroscopic consequences of systematic changes to such constitutive theory.

We consider the reverse impact experiment as a basic ignition to detonation transient. When a piston is driven into a porous mixture, a compaction wave develops and runs faster than the piston interface. The compaction wave increases the pressure, initiates a reaction and as we will show transforms into a self-sustained detonation wave that runs quasi-steadily into the unreacted mixture. The possibility of a sonic state in the following flow is governed by the Rankine-Hugoniot relations for suitable reaction products. The structure of a quasi-steady, self-sustained reactive wave has a precursor front that processes reactant materials with termination in a sonic state in the reaction products, and

is non-classical in the sense that reaction processes are started by compaction processes as opposed to a shock wave which is the case for the classical ZND model of detonation.

For this discussion, we regard the SSD as a detonation in reactive materials that nominally runs at pressures much lower than what is observed in "ideal" explosives. The energy release process is due to mixing and reaction between reactant constituents and is not necessarily contained in molecular explosive grains. We picked the AL/Teflon mixture as a model material because there is a significant amount of data and experiments (see Dolgoborodov et al[2] for example) and specifically experiments have been conducted in Prof. N. Glumac's laboratory at the University of Illinois. The example and attempt to describe Al/Teflon helps us develope a paradigm that allows us to establish a baseline methodology to model a class of reactive materials.

Calculations of the ambient sound speed of AL/Teflon were found to be in the range between $1.14\ km/sec$ and $5.23\ km/sec$ depending on the reactants mass ratio. However from estimates obtained from Cheetah 5.0 thermo-equilibrium software provided by L. Fried and the Lawrence Livermore National Laboratory, we found that typical (sonic) CJ wave speeds were as low as $1.42\ km/sec$, and subsonic relative to the initial ambient reactants. For example, the ambient mixture sound speed for a 45%/55% Al/Teflon mass ratio was $c_0 = 2.33\ km/sec$. If one assumes simply that the wave head is supersonic relative to the ambient, fresh material as is the case for a classical ZND detonation structure for which the wave head is a supersonic shock wave, then there is an apparent dilemma. The resolution is that the lead front ahead of the reaction zone is subsonic and processed by a compaction wave first. The structure that follows is related to energy releasing reaction that terminates on a sonic state or CJ state. But the entire structure is at best quasi-steady since weak hyperbolic precursor must lead the compaction wave structure in such a scenario.

We present calculations that support this scenario in AL/Teflon mixtures. First we develop an analytic solution with the assumption that a pure compaction wave is followed by a reaction wave. Then we develop another analytic solution with the assumption that the reaction and compaction processes occur simultaneously. Finally we carry out a direct simulation of the reverse impact and show clearly that a stable quasi-steady structure is obtained via the compaction and reaction processes that terminate at CJ state estimated by Cheetah.

The Composition of materials, EOS and the Hydrodynamics

We assume our material is a mixture of three constituents: aluminum, Teflon and inert gas. These constituents of the mixture are labeled with letters A, T, and G respectively. The end state products are labeled with a P. The composition of the mixture at any state of reaction and compaction are represented by the values of the volume and mass fractions of the constituents. The volume fraction of the inert gas α represents the degree of compaction of the material, whereas the mass fraction λ of the product is used to represent the amount of conversion from the reactant state to product state. The symbols λ_T and λ_A are the mass fractions of the mixtures to Teflon, aluminum. The symbols ϕ_A, ϕ_T and ϕ_P represent the volume fractions of aluminum, Teflon and the product respectively. The symbols ρ_i and v_i $(i = A, T, G)$ are the densities and specific volumes of aluminum, Teflon and inert gas. The density, specific volume and pressure of the mixture are represented as ρ, v and p respectively.

These quantities for the composition of a mixture should satisfy the following five conditions consistent with standard mixture theory:

Relation Between Composition Variables

$$\begin{cases} \phi_A + \phi_T + \alpha = 1,\ \lambda_A + \lambda_T + \lambda_G = 1 \\ \rho_A\phi_A + \rho_T\phi_T + \rho_P\phi_P = \rho \\ \rho\lambda_A = \rho_A\phi_A,\ \rho\lambda_T = \rho_T\phi_T \end{cases} \tag{1}$$

The unknowns to be specified other than α and λ are $\lambda_A, \lambda_T, \phi_A, \phi_T$, and ϕ_P. We used the following models for the closure to specify those degrees of freedom.

Closure Variables

$$\Phi = \frac{\lambda_A}{\lambda_T},\ \Psi = \frac{v_A}{v_T},\ \Omega(\lambda) = \frac{v_{ps}}{v_p} \tag{2}$$

where $v_{ps} = (v_A\lambda_A + v_T\lambda_T + \alpha v)/(1-\lambda)$ so that $v = v_{ps}(1-\lambda) + v_p\lambda$.

The first two equations (saturation conditions) in equations (1) and the three closures in equations (2) determine $(\lambda_A, \lambda_T, \phi_A, \phi_T, \phi_P)$ as functions of α and λ as follows:

$$\begin{cases} \lambda_T &= (1-\lambda_G-\lambda)/(1+\Phi), \\ \lambda_A &= \Phi\lambda_T \\ \phi_T &= \frac{\Omega(1-\alpha)-\lambda\alpha)}{(1+\Psi\Phi)(\Omega+\lambda)}, \\ \phi_A &= \Psi\Phi\phi_T, \\ \phi_P &= \lambda/(\Omega+\lambda) \end{cases} \tag{3}$$

Mixture Equation of State

We assume that the equation of state (EOS) is represented by the energy $e(p, v, \alpha, \lambda)$ function of pressure p, volume v, α and λ and the EOS is again assumed to be a linear composition of energy functions of each constituent $e_i(p_i, v_i, \alpha)$, $i = A, T, P$. The energy function e_P for the product state is assumed to be independent of α.

To determine the pressures p_A and p_T we assume pressure equilibrium between Teflon and aluminum reactant and use the theory Caroll and Holt [1] to obtain $p_A = p_T = p/(1-\alpha)$. We assume the pressure equilibrium between product and reactant to model the pressure p_G in the EOS as well. The resulting composite energy function is given as follows:

$$\begin{aligned} &e(p, v, \alpha, \lambda) = e_A(\tfrac{p}{1-\alpha}, \tfrac{v\phi_A}{\lambda_A}, \alpha)\lambda_A \\ &+e_T(\tfrac{p}{1-\alpha}, \tfrac{v\phi_T}{\lambda_T}, \alpha)\lambda_T + e_P(p, \tfrac{v\phi_P}{\lambda_P})\lambda \end{aligned} \tag{4}$$

We assume that the functions $e_A(p, v)$ and $e_T(p, v)$ are linear function of pressure p in such a form $e_i(p, v) = e_i^s(v) + v/\Gamma(p - p_i^s(v)$ where $i = A$ or T. Then the mixture energy function e is also a linear function of the pressure p and can be written in the following form:

$$e(p, v, \alpha, \lambda) = A(v, \alpha, \lambda) + K(v, \alpha, \lambda)p \tag{5}$$

The Hydrodynamic Model

The hydrodynamic model with constitutive equations, that include momentum and thermal transport, is represented by the system (6)-(10) of conservation equations for (p, v, u) with two constitutive equations for the progress variables (α, λ),

$$\frac{\partial\rho}{\partial t} + u\frac{\partial\rho}{\partial x} + \rho\frac{\partial u}{\partial x} = 0, \tag{6}$$

$$\rho[\frac{\partial u}{\partial t} + u\frac{\partial u}{\partial x}] = \frac{\partial\sigma}{\partial x}, \tag{7}$$

$$\rho[\frac{\partial e}{\partial t} + u\frac{\partial e}{\partial x}] = \sigma\frac{\partial u}{\partial x} - \frac{\partial q}{\partial x}, \tag{8}$$

$$\frac{d\alpha}{dt} = r_\alpha, \tag{9}$$

$$\frac{d\lambda}{dt} = r_\lambda, \tag{10}$$

where

$$\sigma = -p + \mu(\phi)\frac{\partial u}{dx}, \tag{11}$$

$$q = -k(\phi)\frac{\partial T}{\partial x}, \tag{12}$$

$$r_\alpha = -k_\alpha(A(p-p_0) + (\alpha-\alpha_0)), \tag{13}$$

$$r_\lambda = \begin{cases} k_\lambda(\frac{p}{p_{cj}})^\mu(\hat{\lambda}-\lambda)^\nu, & \text{if } p > \tilde{p} \\ 0, & \text{otherwise,} \end{cases} \tag{14}$$

and T is temperature.

The system of equations (6)-(10) can be written in conservative form as follow:

$$\frac{\partial\mathbf{U}}{\partial t} + \frac{\partial\mathbf{F}}{\partial x} = \mathbf{S} \tag{15}$$

$$\mathbf{U} = \begin{bmatrix} \rho \\ \rho u \\ \rho E \\ \rho\phi \\ \rho\lambda \end{bmatrix}, \mathbf{F} = \begin{bmatrix} \rho u \\ \rho u^2 + p \\ \rho u(E + p/\rho) \\ \rho u\phi \\ \rho u\lambda \end{bmatrix},$$

$$\mathbf{S} = \begin{bmatrix} 0 \\ \frac{\partial}{\partial x}(\tilde{\sigma}) \\ \frac{\partial}{\partial x}(u\tilde{\sigma} - q) \\ \rho r_\phi \\ \rho r_\lambda \end{bmatrix}$$

where $\tilde{\sigma} = \mu(\phi)\frac{\partial u}{\partial x}$ and $E = e + u^2/2$.

Steady State Structure

For a steady wave speed $D > 0$ for a wave moving into the fresh region with $u = 0, p = p_0, \rho = \rho_0$, define the spatial coordinate $n = x - Dt$. Let the particle velocity in the steady wave frame be $U = u - D$. Then with $\frac{\partial}{\partial t} = 0$ the equations (6)-(8) become,

$$m(U+D)+(p-p_0)=\mu\frac{dU}{dn} \tag{16}$$

$$\mathcal{H}=\mathcal{H}_0+U\mu(\phi)\frac{\partial U}{dn}+k(\phi)\frac{\partial T}{\partial n} \tag{17}$$

where $\mathcal{H}=m[e+\frac{1}{2}U^2+pv]$, $\mathcal{H}_0=m[e_0+\frac{1}{2}(u_0-U)^2+p_0v_0]$ and $m=\rho U=\rho_0(u_0-D)$.

The ODE system for the steady state can be written as a system of two equations,

$$\frac{dU}{dn}-\frac{1}{m\mu K}\left(k(\phi)\frac{dT}{dx}\right)=\Phi, \tag{18}$$

$$\frac{d\alpha}{dn}=\frac{r_\alpha}{U} \tag{19}$$

where

$$\Phi=-\frac{(p_0-mu_p)(K+v)+(A+\frac{1}{2}U^2-\mathcal{H}_0)}{\mu(\phi)K}$$

and $v=1/\rho$. In the expression for Φ, we used the form of EOS $e(p,v,\alpha,\lambda)$ given in equation (5).

There are two equilibrium points for the system of ODE at (u_p,α^*) and $(0.0,\alpha_0)$. The first point is the admissible inert steady state ($*$-state) obtained from the Hugoniot analysis with equation (19) and the second point is the ambient state. It is observed from the numerical simulation that the ambient state is a saddle point of the system and the $*$-state is sink point of the system as reported by Stewart [5] $et.al$. Therefore the ODE is solved from a state of small perturbation to the ambient state until the trajectory reaches the $*$-state. We note the value of the piston velocity u_p and the viscosity coefficient μ can potentially have a strong effect on the stability of the solution of the ODE.

Simple, phenomenological forms have been selected for the compaction rate law and the reaction rate law in the absence of detailed rate information. We anticipate that in future works these forms will be provided by mesoscopically motivated models. The pressure $\tilde{p}$ in equation (14) is the threshold of pressure for the initiation of reaction from compaction process and it is set to zero for the illustration in the next section. The value $\hat{\lambda}$ in the same equation indicates that there can be a limit in the reaction process but we also set that to 1.0 in this paper.

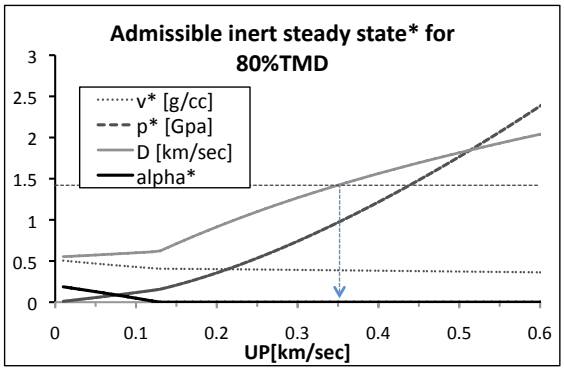

Fig. 1. EQB compaction wave structures of velocity D, pressure p, specific volume v and porosity variable α versus u_p, according to Rankine-Hugoniot analysis.

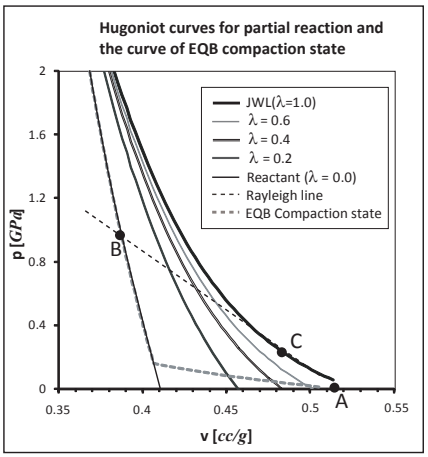

Fig. 2. Partially reacted $p-v$ Hugoniot curves for $\lambda\in[0,1]$ from left to right (solid curves) and the curve of fully compacted inert steady states (dotted curve)

Self-Sustained, Low-Speed, Subsonic Detonation Waves

In this section, we demonstrate the existence of a low-speed, self-sustained detonation that is an admissible solution of the hydro-dynamic model presented by (6) - (10). The closure variables for this purpose are chosen as follows,

$$\Phi = \frac{\lambda_A}{\lambda_T} = \frac{\lambda_A^0}{\lambda_T^0},\ \Psi = \frac{v_A}{v_T} = \frac{v_A^0}{v_T^0},\ \Omega(\lambda) = 1 - \lambda \ . (20)$$

The admissible inert steady wave solutions of the system can be obtained using the relation for both compaction and reaction equilibrium $r_\alpha = 0$ and $r_\lambda = 0$ instead of using equations (9) and (10) in the system. (See Stewart et al [5] for the details). In the following displayed figures we assume the constants for the rate of compaction (equation (13)) are $k_\alpha = 10\mu sec^{-1},\ p_0 = 1\ atm, \alpha_0 = 0.2$. The admissible inert steady state solution versus piston velocity u_p is shown in Figure 1.

For the demonstration purpose, we assume that we are given an 80% TMD aluminum and Teflon mixture that is mixed at 45:55 mass ratio. The product equation of state for the mixture is computed in the form of JWL EOS $e(p,v) = e^s(v) + \frac{v}{\omega}(p - p^s(v))$, where

$$\begin{aligned} p^s(v) &= Ae^{-R_1 V} + Be^{-R_2 V} + CV^{-(\omega+1)} \\ e^a(v) &= -\rho_0 \int p^s(V) dV \end{aligned} \quad (21)$$

and $A = 496.79\,\text{GPa}, B = -3.61\,\text{GPa}, C = 0.09\,\text{GPa}, R_1 = 7.0, R_2 = 2.0, \omega = 0.079, V = v/v_0$ and $v_0 = 0.51389\ [g/cc]^{-1}$.

The $p-v$ Hugoniot curves of all partially reacted ($\lambda < 1$) and fully reacted product ($\lambda = 1$) EOS and the Rayleigh line are shown in Figure 2. We also added the admissible, inert steady state solutions on the p-v plane in Figure 2. Note that the portion of inert solutions $\alpha^* = 0$ overlaps the Hugoniot of reactant.

The intersection (marked as B) of the Rayleigh line with the admissible solution curve represents a steady inert (unreacted) state solution of the system (6) - (10). Therefore if we assume that there is no reaction until the material is fully compacted, then the structure of a possible solution of our system can be obtained by joining the solution of the inert compact wave and the reaction wave solution starting from the compacted wave solution to the burnt product. These two wave solutions can be computed separately using Hugoniot relation and the ordinary differential equations for equations (9) and (10) respectively. (For more details regarding the steady wave analysis types, see Stewart et al[5]). For an illustration of the features of the model in this paper, we removed the momentum and thermal transport terms in the governing equations ($\mu = k_T = 0$). Figure 3 presents the solution of this type. In the figure, state **0** is the ambient state (same as **A** in Figure 4), state **1** is the compacted inert state and **2** (state **B** in Figure 4) is the burnt product state which is the state **C** in Figure 4.

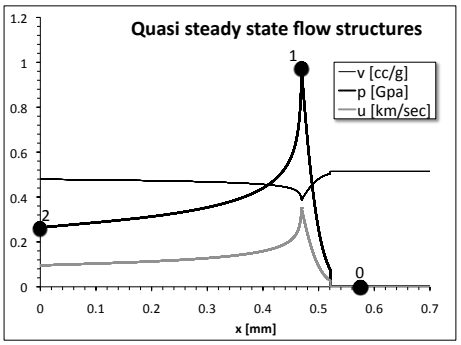

Fig. 3. Steady state flow structure with assumption that the reaction initiates after full compaction.

Figure 4 shows the steady state solution with the assumption that the reaction and compaction start at the same time. In this case the two ODEs (9) and (10) together with the Hugoniot relations are solved simultaneously. The peek pressure in this case occurs at the partially reacted state ($\lambda \approx 0.6$).

Finally, we carried out the reverse impact simulation numerically on a bed of initially unreacted mixture with its reactant composition described by solving the full system of equations (15). We start the numerical simulations at the time ($t = 0$) when a $3mm$ bed ($-2\ mm \leq x \leq 1.0\ mm$) is impacted against a stationary wall (the piston surface located at $x = 1.0mm$) at a constant velocity $u_p = 60m/sec$. Therefore the particle velocity in the bed at the impact time is same as the impact velocity with a reflective boundary condition at the impact location. For this simulation we used the heat transfer coefficient $k_T = 0.0002$ and the viscosity coef-

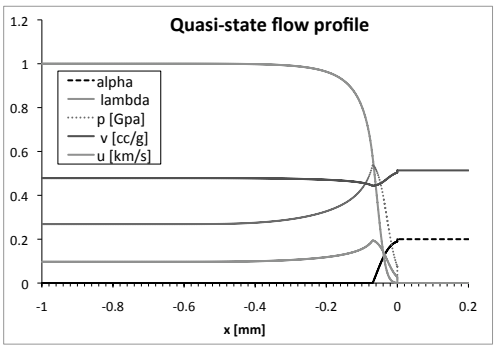

Fig. 4. Combined quasi-state flow field. The length of compaction state is about 0.07 mm and the reaction length is about 0.7 mm.

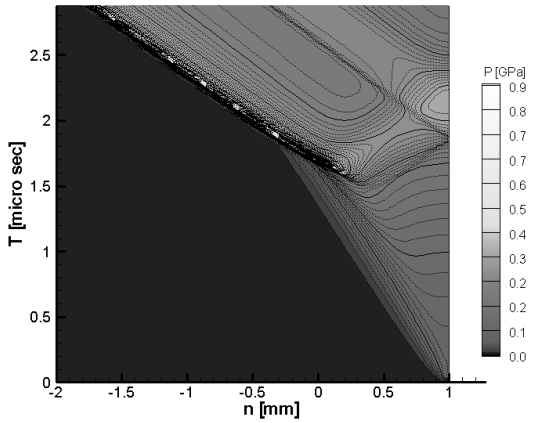

Fig. 5. The x-t plot of pressure field from the reverse impact simulation. $u_p = 60\, m/sec$, $\mu = 10^4\ P$ and $k_T = 0.0002$.

ficient $\mu = 0.0001$.

Figure 5 shows the space-time plot of pressure field generated from this simulation. We see that the steady state detonation shock develops at around $t = 2.0\mu sec$. We see from the result, very similar wave transitions reported by Saenz *et. al.*[4], specifically a compaction wave forms followed by, detonation wave (D_1 in Saenz and Stewart[4]) in the compacted material. Figure 8 shows the x-t plot of the volume fraction α from the same simulation and that when the detonation starts, the area behind the front of detonation shock and inside the plug[5] are fully compacted. The final detonation wave that propagates in the unperturbed material shown in the figure is quasi-steady, self-sustained and subsonic ($D = 1.39km/sec$) relative to the sound speed of ambient state ($c_0 = 2.33\ km/sec$).

It also clearly shows the scenario of the transition from deflagration to detonation (DDT) as follows:

(1) A compaction wave starts to develop due to the impact on the material at the right end.

(2) The reflected wave compresses the material starting a very weak reaction. Figure 6 shows wave profiles at time $t = 0.5, 1, 1.5$ and $2.0\,\mu sec$. This figure shows that before significant reaction occurs with $\lambda < 0.2$). If the material does not react, the bed will be remained partially compacted with ($\alpha = \alpha^* \approx 0.11$).

(3) But the reaction wave staring at the impact location through a region of about 90% compaction pushes from behind and then eventually make a full compacted spot. The full compaction does not start at the impact point $x = 1.0$ but inside the bed at around $x = 0.5$ as shown in the figure which is called a plug[5]. In Figure 6, the region ($0.3 < x < 0.5$) is the place of the plug at time $t = 1.5\mu sec$.

(4) Once a plug is developed, starting at the front of the plug, the material reacts rapidly. Figure 7 presents the situation clearly. It shows the wave profile of mass fraction λ which is our variable for the reaction process at various time t. In this Figure, we see after time $t = 1.5\mu sec$, the change in λ is dramatically. But note that behind the plug area, the reaction still does not develop as quickly as its front. So we see that the plug in fact acts like a virtual piston as described by Stewart et. al[5] in order to make a detonation to occur shortly after then.

(5) The width of plug grow rapidly and the completion of reaction occurs in the whole region behind the front of plug: Detonation occurs.

Figure 8 shows the time-space (xt) plot of the variable α to show the whole time history of compaction mechanism of this simulation. It clearly shows three region: compaction wave, reaction behind the compaction wave and the complete reaction area behind detonation and plug.

Effect of Viscosity and Heat Transfer on the Reaction on the System

Next we illustrate the effect of viscosity and heat conduction in the bed. To see the effect clearly, we carried out reverse impact simulation with higher

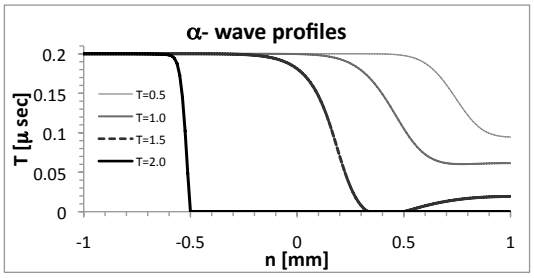

Fig. 6. Wave profile of volume fraction (compaction rate) at time $t = 0.5, 1.0, 1.5$ and 2.0 μsec.

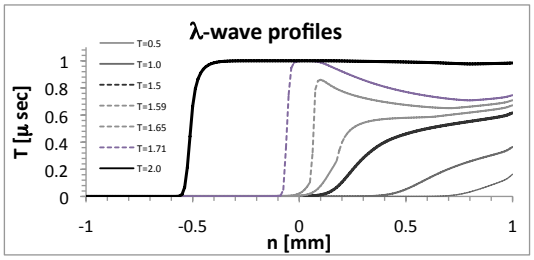

Fig. 7. Wave profile of mass fraction λ.

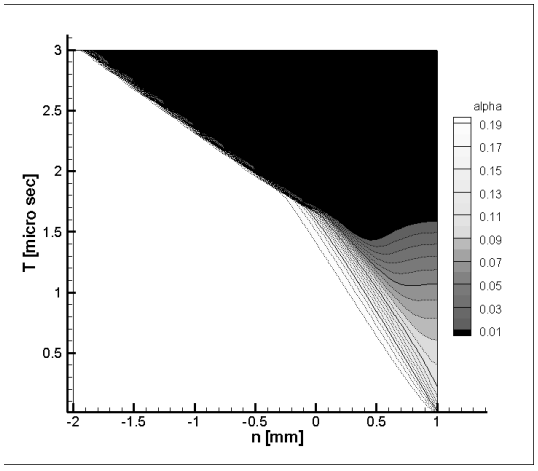

Fig. 8. The x-t plot of α field from the reverse impact simulation. $u_p = 60m/sec$, $\mu = 10^4$ P and $k_T = 0.0002$.

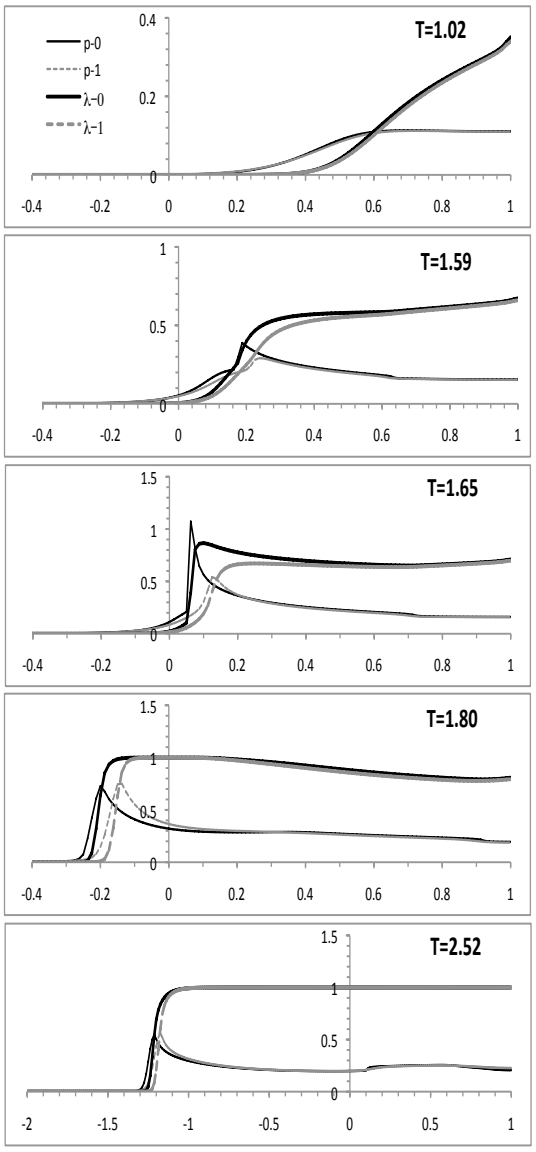

Fig. 9. The effect of viscosity and heat transfer ($\mu = 0.03, k_T = 0.005$). The black and gray colored curves in the series of the figures are the λ(thick-curves) and p (thin-curves) profiles with (black) and without (gray) these effects. The reaction is significantly delayed due to the effect of heat release and viscosity after a plug is formed. But the defect is healed as a steady state detonation develops.

values of viscosity and heat transfer coefficients $\mu = 0.03$ and $k_T = 0.005$. But these values can not be increased arbitrarily large due to the occurrence of instability in the system. Figure 9 presents the wave profiles of pressure p and mass fraction λ with transfer coefficients μ and k_f (marked by $p-1$ and λ_1) and without these transfer effect (marked by $p - 0$ and λ_0 in the legend of second plots). From this numerical experiment, we observed that the presence of heat transfer and viscosity does not play an important role on the flow structures until a plug is formed as seen in the wave profile at $t = 1.02$ in Figure 9. These wave profiles are very similar to each other.

Once the plug is formed (at around $t = 1.59\,\mu sec$), the reaction is significantly delayed due to the effect of viscosity and heat transfer mechanism as seen in the figure for time $t = 1.59$ to $t = 1.8\,\mu sec$. But eventually as a steady state detonation begins to develop, the defect heals as the effect of transport is restricted to a very thin region as can be seen in the profiles at time $t = 2.52\,\mu sec$. Therefore we conjecture that the importance of transport might be crucial in understanding transition behaviors, as it might play a lesser role in the early phase of the compaction wave (with weak reactions) and the final detonation wave structure.

Conclusion

We presented a simple hydrodynamic model that admits a solution of a quasi-steady, self-sustained reactive wave that is formed from a compaction wave followed by a reaction zone of products. This non-classical 'solid' detonation wave structure is subsonic relative to the sound speed in the ambient state. The wave head is actually comprised of a subsonic compaction wave. These early studies have been concerned mainly with a purely hydrodynamic model with simple heat release and viscosity effects, and phenomenological compaction rate and reaction rate laws. We have confirmed all the essential analytically derived conclusions by direct numerical simulation, and we observed that the quasi-steady wave structure does indeed emerge via a scenario that is very similar to the more well known DDT mechanism that has been described in porous material reported by previous researchers[5, 4]. Near term plans include continued investigation of the effect of the viscosity effect and heat release on the compaction and inclusion of more complex constitutive relations that are derived from meso-scopic consideration of the underlying kinetics and intra-material transport.

Acknowledgments

Supported by the US Air Force Research Laboratory, Munitions Directorate F08630-00-1-0002, and the Air Force Office of Scientific Research, Mathematics FA9550-06-1-0044, and the Office of Naval Research.

References

1. Carroll, M. and Holt, A. . Static and Dynamic Pore-Collapse Relations for Ductile Porous Materials. *JOURNAL OF APPLIED PHYSICS*, 43:1626, Jan 1972.

2. Dolgoborodov, A. Y. , Makhov, M. N. , Kolbanev, I. V. , Streletskii, A. N. , and Fortov, V. E. . DETONATION IN METAL–TEFLON MECHANOACTIVATED COMPOSITES. *International detonation symposium*, page 8, Sep 2006.

3. Eakins, D. and Thadhani, N. . The Shock Compression of Reactive Powder Mixtures. *Invited Review Article, International Materials Reviews*, 54(4):181–213, 2009.

4. Sáenz, J. A. and Stewart, D. S. . Modeling deflagration-to-detonation transition in granular explosive pentaerythritol tetranitrate. *Journal of Applied Physics*, 104(4):043519–+, Aug. 2008.

5. Stewart, D. S. , Asay, B. W. , and Prasad, K. . Simplified modeling of transition to detonation in porous energetic materials. *Physics of Fluids*, 6:2515–2534, July 1994.